Iranian Int. J. Sci. ***5****(1), 2004, p.91-105*

On the Analytic Minimum Information Deconvolution Technique, Its Implication on Random Noise Elimination and Moho Phase Detection

Javan G. Doloei[1], M. Mokhtari[1] and D. Dyrelius[2]
[1] *Seismology Research Center, IIEES, Tehran, IRAN*
[2] *Geophysics Dept., Uppsala University, Uppsala, Sweden*
(received: 7/12/2003 ; accepted: 7/5/2004)

Abstract

A reflection seismogram can be represented as a convolution of a source wavelet with a set of reflection coefficients. In a standard model these coefficients are scalar and real impulses. For all plane waves, displacements are phase shifted in post-critical angles. In this case reflection coefficients can be complex and the scalar deconvolution does not remove distortions perfectly. To overcome this problem, it has been attempted to examine an analytical technique [i.e. Analytic Minimum Information Deconvolution (AMID)] that can remove distorted effects from seismograms. The necessary codes have been written for applying AMID technique to synthetic and real data. Using computer programs in seismology (Herrmann, 1996), the necessary synthetic seismograms are generated for a specific structural earth model. 10% random noise is added to the synthetic seismograms and the output of AMID filter is investigated for different source - receiver offsets. The results of this study shows the ability of AMID for elimination of random noise and Moho phase detection.

Keywords: *Analytic minimum information, seismic reflection, synthetic seismogram, random noise, Moho phase detection.*

Introduction

In seismic studies, the earth is assumed as a homogeneous layered media. In such a simple earth model, a typical seismogram can be modeled as the convolution of a source wavelet with a set of scalar and real coefficients.

For wide – angle reflections or curved wavefront standard deconvolution techniques no longer are valid for crustal scale of seismic data. The above conditions will result in post-critical reflection observations. Due to the creation of inhomogeneous /interface waves at the boundary of layers (Aki and Richards, 1985), reflection coefficients can be complex.

The analytic method to deconvolve complex wavelets of seismic reflection data was introduced by Levy and Oldenburg (1982) by means of the linear inverse theory. The practical analytic formulation for complex version of minimum entropy deconvolution was developed by Ulrych and Walker (1982). Claerbout (1978) developed the Minimum Information Deconvolution (MID) method. MID technique uses an iterative gradient descent algorithm, to achieve the convergence of the solution. Kim and Marillier (1996) drove a complex version of MID to deconvolve ocean bottom seismometer (OBS) data. The main purpose of this article is to extend the Analytical Minimum Information Deconvolution (AMID) technique to synthetic and real examples of deep seismic data.

Theoretical Backgrounds

If a plane P-wave is traveling with horizontal slowness S in direction x, then the displacement of scattered upgoing P-waves from Moho boundary can be rewritten as [e.g. Arons and Yennie, 1950; Aki and Richards, 1985]:

$$S(\sin i_1, 0, -\cos i_1) P_M P \exp[i\omega(Px - \frac{\cos i_1}{\alpha_1} z - t)] \qquad (1)$$

where i_1 is incidence angle and $P_M P$ is reflection of P-wave at the Moho discontinuity. The reflection/refraction rays of an incident P-wave in a case of post-critical angle is shown in Figure1. In general, reflection coefficient of $P_M P$ can be written as:

$$P_M P = [(b\frac{\cos i_1}{\alpha_1} - c\frac{\cos i_2}{\alpha_2})F - (a + d\frac{\cos i_1}{\alpha_1}\frac{\cos j_2}{\beta_2})HP^2]/D \qquad (2)$$

Where a, b, c, and d describe the relation between shear velocities and densities. E, F, G, and H are constant parameters to relate shear and

compensational velocities to cosine directions. The factor D and ray parameter, P are as follow:

$$D = EF + GHP^2$$

$$P = \frac{\sin i_1}{\alpha_1} = \frac{\sin j_1}{\beta_1} = \frac{\sin i_2}{\alpha_2} = \frac{\sin j_2}{\beta_2} \tag{3}$$

In the following, reflected P-waves beyond the critical angle (i.e. *post critical angle*) have been evaluated. In equation (2) if the incidence angle $i_1 = i_p > i_c = Arc\sin(\frac{\alpha_1}{\alpha_2})$, then i_2 (the angle of transmitted wave) becomes complex because it has been assumed that $\alpha_2 > \alpha_1$.

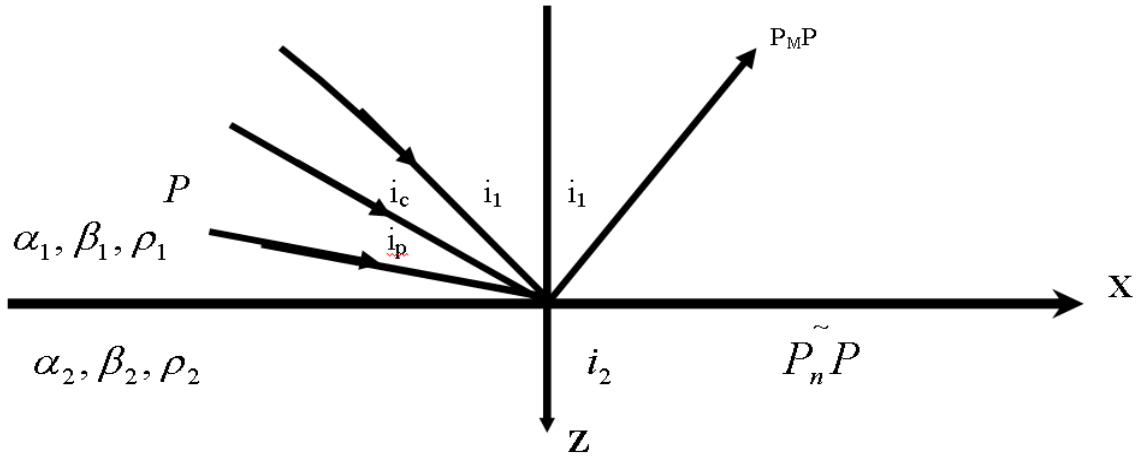

Figure 1. Notation for reflection at the Moho border. α, β and ρ is compress ional wave velocity, shear wave velocity and density, respectively. a- Incidence angle i_1 < i_c (critical angle). b- $i_1 = i_c(Arc\sin(\alpha_1/\alpha_2)$ and $i_2 = 90^\circ)$. c- $i_1 = i_p > i_c$, that $\tilde{P_n}P$ wave acts as an inhomogeneous /interface wave and decays exponentially with depth.

$$\cos i_2 = -i(\sin^2 i_2 - 1)^{1/2} = -i[(\frac{\alpha_2}{\alpha_1}\sin i_p)^2 - (\frac{\alpha_2}{\alpha_1}\sin i_c)^2]^{1/2}$$

$$= -i(\frac{\alpha_2}{\alpha_1})(\sin^2 i_p - \sin^2 i_c)^{1/2} \tag{4}$$

$$\cos j_1 = (1-\sin^2 j_1)^{1/2} = (1-\beta_1{}^2 P^2)^{1/2} \quad (5)$$

$$\cos j_2 = (1-\beta_2{}^2 P^2)^{1/2} \quad (6)$$

To rewrite equation (2) based on relations (4), (5) and (6):

$$\begin{aligned}
\tilde{P}nP = \{&[b\frac{\cos i_p}{\alpha_1}(\frac{b}{\beta_1}\sqrt{1-\beta_1{}^2P^2}+\frac{c}{\beta_2}\sqrt{1-\beta_2{}^2P^2}) - aP^2(a+d\frac{\cos i_p}{\alpha_1\beta_2}\sqrt{1-\beta_2{}^2P^2})]\\
&+i[\frac{c}{\alpha_1}(\sin^2 i_p-\sin^2 i_c)^{1/2}(\frac{b}{\beta 1}\sqrt{1-\beta_1{}^2P^2}+\frac{c}{\beta_2}\sqrt{1-\beta_2{}^2P^2})\\
&+d\frac{P^2}{\alpha_1\beta_1}(a+d\frac{\cos i_p}{\alpha_1\beta_2}\sqrt{1-\beta_2{}^2P^2})(\sin^2 i_p-\sin^2 i_c)^{1/2}\sqrt{1-\beta_1{}^2P^2}\,]\}\\
\times\{&[b\frac{\cos i_p}{\alpha_1}(\frac{b}{\beta_1}\sqrt{1-\beta_1{}^2P^2}+\frac{c}{\beta_2}\sqrt{1-\beta_2{}^2P^2})+ap^2\\
&+ap^2(a-d\frac{\cos i_p}{\alpha_1\beta_2}\sqrt{1-\beta_2{}^2P^2})]\\
&+i[d\frac{P^2}{\beta_1}\sqrt{1-\beta_1{}^2P^2}(\sin^2 i_p-\sin^2 i_c)^{1/2}(a-d\frac{\cos i_p}{\alpha_1\beta_2}\sqrt{1-\beta_2{}^2P^2})\\
&-\frac{c}{\alpha_1}(\sin^2 i_p-\sin^2 i_c)^{1/2}(\frac{b}{\beta_1}\sqrt{1-\beta_1{}^2P^2}+\frac{c}{\beta_2}\sqrt{1-\beta_2{}^2P^2})\,]\}^{-1}
\end{aligned} \quad (7)$$

A suit equivalent for equation (7) will be in the following form:

$$\begin{aligned}
\tilde{P_n}P &= \frac{A_{1p}+iA_{2p}}{B_{1p}+iB_{2p}} = (\frac{A_{1p}B_{1p}+A_{2p}B_{2p}}{B_{1p}{}^2+B_{2p}{}^2}) + i(\frac{A_{2p}B_{1p}-A_{1p}B_{2p}}{B_{1p}{}^2+B_{2p}{}^2})\\
&= A_p + iB_p = \sqrt{A_p{}^2+B_p{}^2}\exp\{i[Arc\tan(\frac{B_p}{A_p})]\}
\end{aligned} \quad (8)$$

Therefore the $\tilde{P_n}P$ interface wave contains both real and imaginary parts. Considering this result, it can be seen that $\tilde{P_n}P$ is written as a function of amplitude, $R_p (= \sqrt{A_p{}^2+B_p{}^2})$ and phase,

$\varphi_p (= Arc\tan(\frac{B_p}{A_p}))]$. Moreover, It should be noted that, due to A_p and B_p are functions of $\alpha_1, \alpha_2, \beta_1, \beta_2, \rho_1, \rho_2$ and i_p, the values of amplitudes and phases depend on elastic parameters. Considering equation (8), equation (1) changes to:

$$S(\sin i_p, 0, -\cos i_p) R_p \exp\{i[\omega(Px - \frac{\cos i_p}{\alpha_1} z - t)] + \varphi_p\} \qquad (9)$$

That is, displacement of reflected up going P-wave is phase shifted by φ_p for $i_p > i_c$.

Therefore, it can be concluded that the pulse shape of the reflected wave is not the same as that of the incident wave. It means that reflected pulse shape is distorted and the amount of distortion depends on the phase φ_p of the complex reflection coefficient. Considering equation (8), The range of phase shift of reflected P-waves have calculated in terms of incidence angle for a simple model that, results have illustrated in Figure 2.

The Seismogram Model and Analytic Convolution

The seismogram $\{ X(t)$; t = 1, NX$\}$ can be modeled as the real part of the convolution of the analytic source wavelet $\{ \hat{W}(t)$; t =1, NW$\}$ with the complex reflectivity function $\{ \hat{Y}(t)$; t = 1, NY$\}$, that is

$$X(t) = \mathrm{Re}[\hat{W}(t) * \hat{Y}(t)] + \hat{n}(t) \qquad (10)$$

Where $\hat{n}(t)$ is the additive noise, and $\hat{W}(t) = W(t) - iH[W(t)]$ and complex reflectivity function $\hat{Y}(t)$ is:

$$\hat{Y}(t) = \sum_j y_j \exp(i\varepsilon_j)\delta(t - \tau_j) \qquad (11)$$

which represents a set of complex coefficients with modulus y_j, phase angle ε_j and delay time τ_j (Kim and Marillier, 1996).

Deconvolution can be defined as the process of extracting the reflectivity function from the seismic trace to improve the vertical resolution and recognition of events (Levy and Oldenburg, 1982).

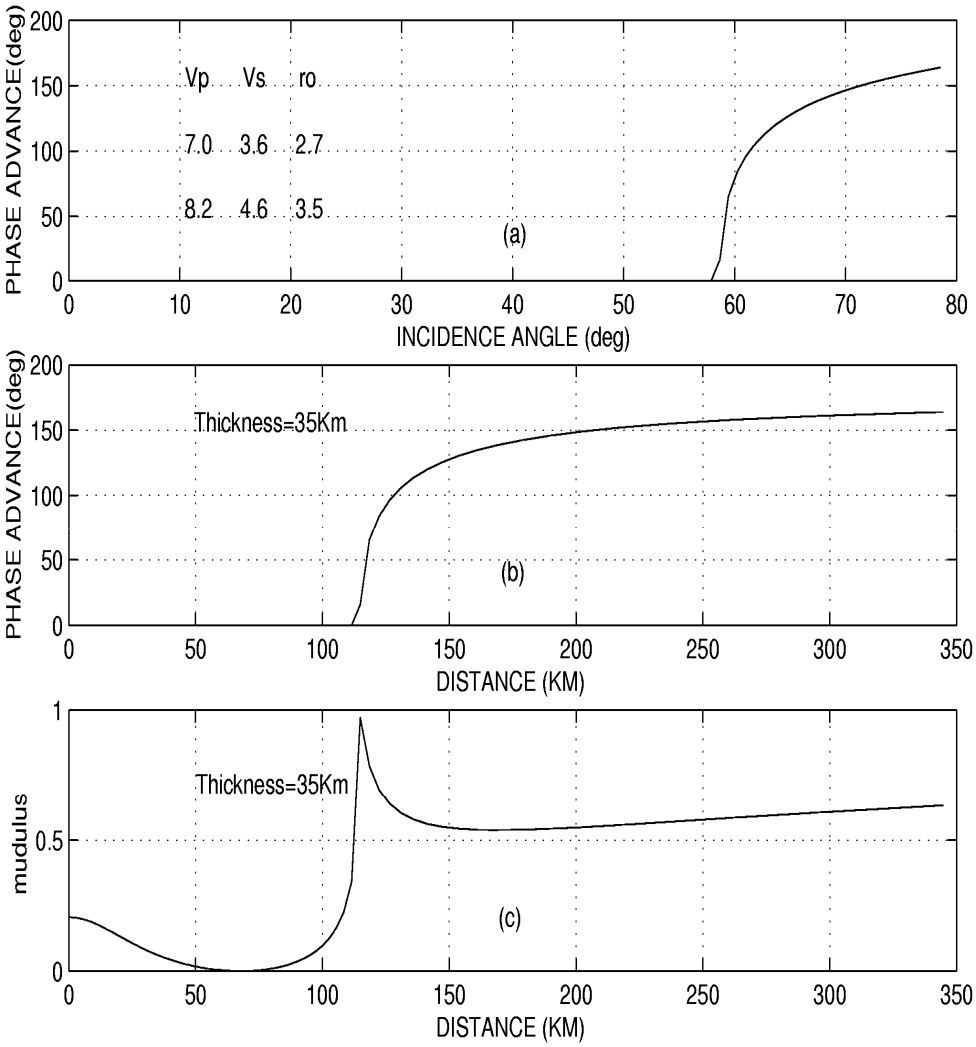

Figure 2. Phase advance of reflected P-waves in one layer model. a) Phase advance versus incidence angel; b) Phase advance versus source-receiver distance; c) Reflection coefficients in terms of source-receiver distance.

Analytic Minimum Information Deconvolution(AMID) Algorithm

The analytic minimum information deconvolution filter $\{\hat{a}(t)\}$ can be written as:

$$\hat{Y}(t) = \hat{X}(t) * \hat{a}(t) \qquad (12)$$

Which $\hat{Y}(t)$ is deconvolved seismogram and the observed seismogram is $X(t)$. Clarebout (1978) presented a complete solution method of scalar MID and a brief of procedure to derive AMID filter $\hat{a}(t)$ is introduced by Kim and Marillier (1996). The equation (12) of Kim and Marillier (1996) can be written as:

$$\sum_t X(t-m+1)X(t-k+1)\sum_m d\hat{a}(m) = -\lambda\sum_t g(t)X(t-k+1) \quad (13)$$

Where λ is the scalar gain factor, $g(t)$ is written as:

$$g(t) = \frac{1}{N}\frac{\hat{Y}(t)}{(\hat{Y}^c(t)\hat{Y}(t))} \quad (14)$$

That superscript c denotes the conjugate.

The ***auto correlation*** function of $X(t)$ can be introduced as vector *A*:

$$A = \sum_t X(t-m+1)X(t-k+1)$$

And the ***cross correlation*** of $g(t)$ and $X(t)$ as vector *B*:

$$B = \sum_t g(t)X(t-k+1)$$

Then equation (13) can be rewritten as

$$f = -\lambda\frac{A^T B}{A^T A} \quad (15)$$

Where f is a vector of filter coefficients of $d\hat{a}(t)$ and $\lambda = \gamma/(\eta.s^{1/2})$. That γ is the predetermined amount of perturbation to the previous filter. It is being changed as the iteration proceeds by the relation (16):

$$\gamma = 0.3(0.1)^{((iter-1.)/niter)} \quad (16)$$

And η is a constant (in the range of 1.0 ~ 3.0) and parameter s is convergence criterion, which it could be calculated as:

$$s = \frac{\sum d\hat{y}(t).d\hat{y}^c(t)}{\sum \hat{y}(t).\hat{y}^c(t)} \tag{17}$$

It should be noted that the assumption $d\hat{y}(t) = X(t) * d\hat{a}(t)$ is considered instead of $d\hat{y}(t)$. Thus the $\hat{a}(t)$ by $\hat{a}(t) = \hat{a}(t) + d\hat{a}(t)$ can be renewed until convergence has been achieved.

Deconvolution algorithms can be used in a series in which one operation removes one type of distortion and is then followed by a different type of deconvolution algorithm to remove another. In seismic data processing, deconvolution is commonly used to attenuate multiple reflections and random noise effects, which leading to an enhanced seismic record.

Application of AMID to Synthetic and Real Data

To illustrate the capability of analytic deconvolution method, the AMID algorithm has been applied to different type of seismograms.

Separating noise from signal is an important subject in geophysics. Many seismic data, especially those acquired on land, are seriously contaminated with noise that impedes interpretation and interferes with further processing and analysis. Noise may be either random or coherent. Random noise is a noise that has no predictability from one trace to the next. Seismic data often has a background of this random noise. This random noise is recognized by its dissimilarity from trace to trace. Seismic signals, on the other hand, are recognized by their lateral continuity, and this continuity is used to distinguish events of interest from the background random noise. Much of this continuity results from the sedimentary character of the data being considered. Eliminating background noise from a seismic trace makes the recognizing of reflections significantly easier, especially when noise is strong.

Using computer programs, synthetic seismograms corresponding with one layer model of Figure 3 have been generated in which are shown in Figs.4 and 7. Since real seismic traces are often associated with background noise, therefore 10% random noise has added to the

generated synthetic seismograms of the first three receivers with offset 100Km, 110Km, and 120km, respectively (Fig.5). Then three consecutive traces of Figure 5 have been deconvolved simultaneously by AMID algorithm, which their results have demonstrated in Figure 6.

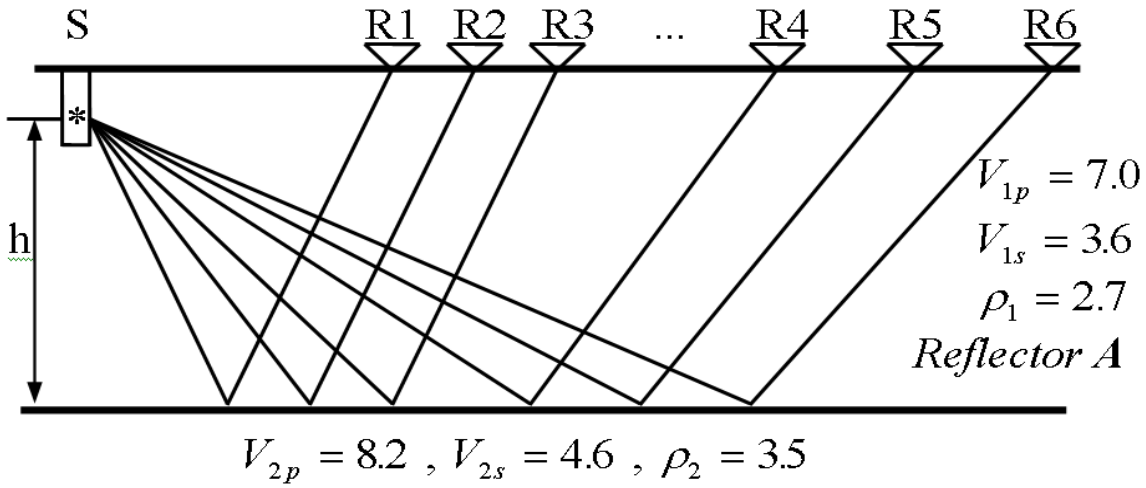

Figure 3. Diagram of one layer model to generate reflected waves from reflector A. h = 35Km, source depth = 100m, $\overline{SR1} = 100km$, $\overline{R1R2} = \overline{R2R3} = 10km$, $\overline{SR4} = 170km$, **and** $\overline{R4R5} = \overline{R5R6} = 20km$. **Dimensions of Velocities and density are in terms of km/sec and g/cm^3, respectively.**

Then 10% random noise has been added to synthetic seismograms of second three receivers (Fig.7), which are shown in Figure8. In this case, the result of AMID output is presented in Figure9.

Results of AMID technique that presented in Figures 6&9 indicate an efficient application of analytical deconvolution to remove distortion and random noise from seismograms.

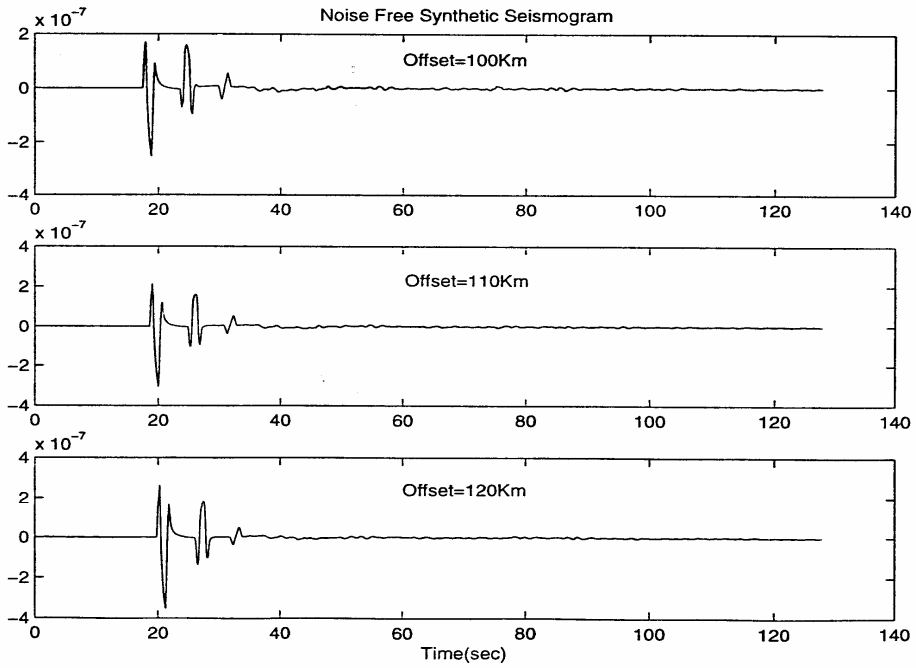

Figure 4.The first group of synthetic reflected waveforms from model of Figure 3.

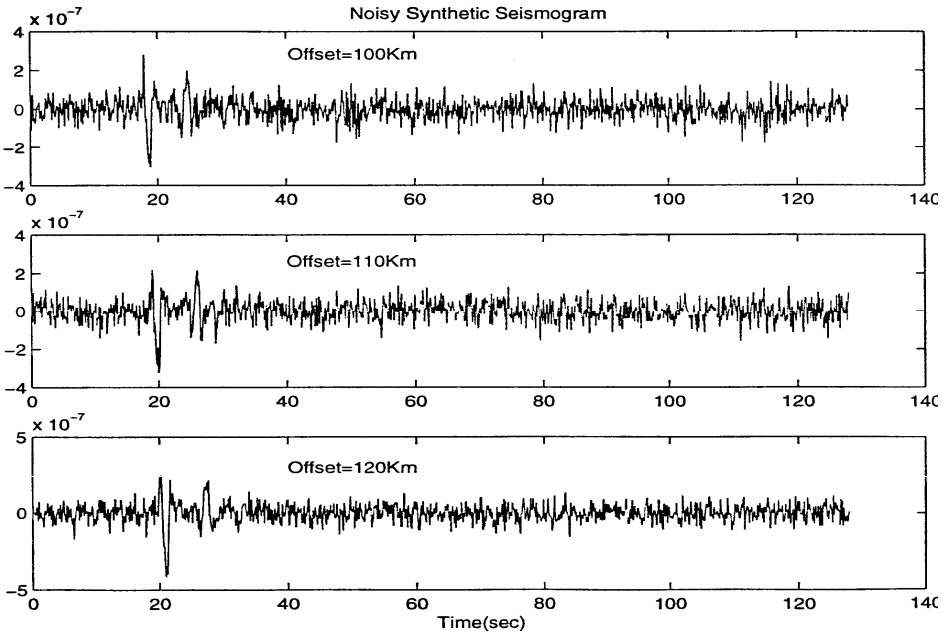

Figure 5. Synthetic seismograms of Figure 4 with additional 10% random noise.

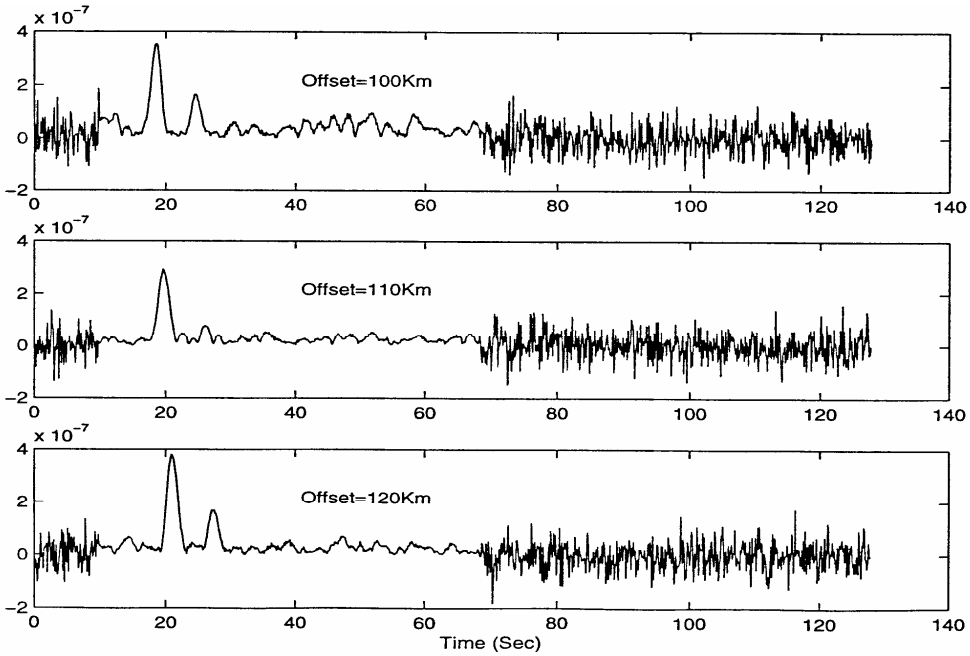

Figure 6. AIMID output on noisy synthetic seismograms of Figure 5.

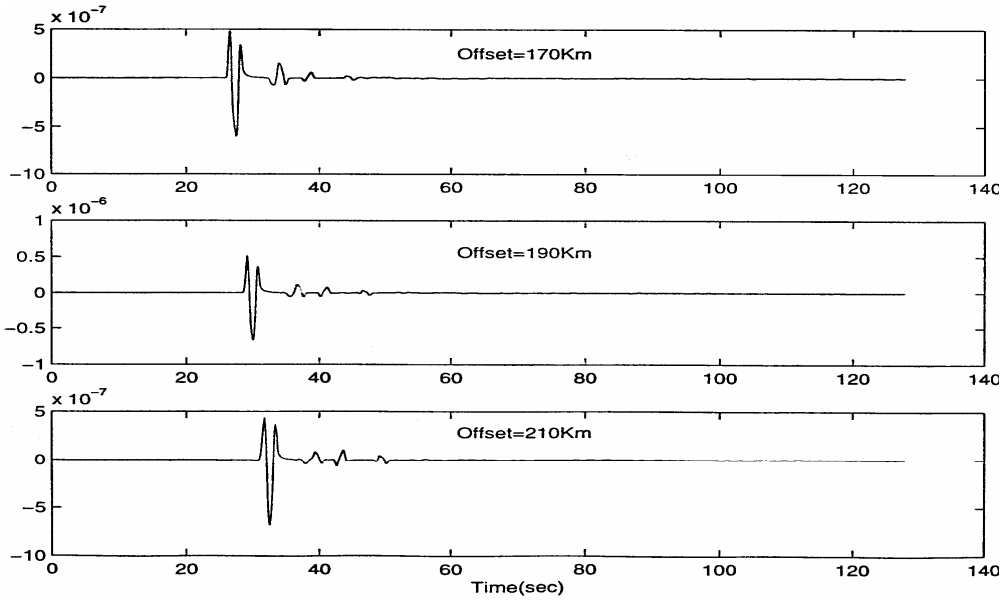

Figure 7. Second group of synthetic reflected waveforms from model of Figure 3.

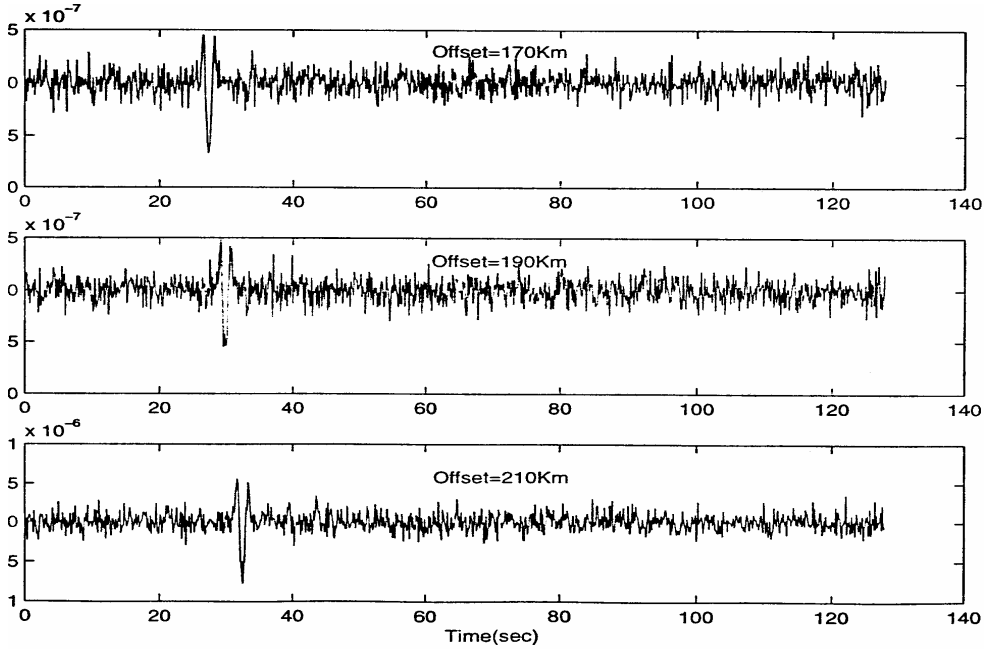

Figure 8. Synthetic seismograms of Figure 7 with additional 10% random noise.

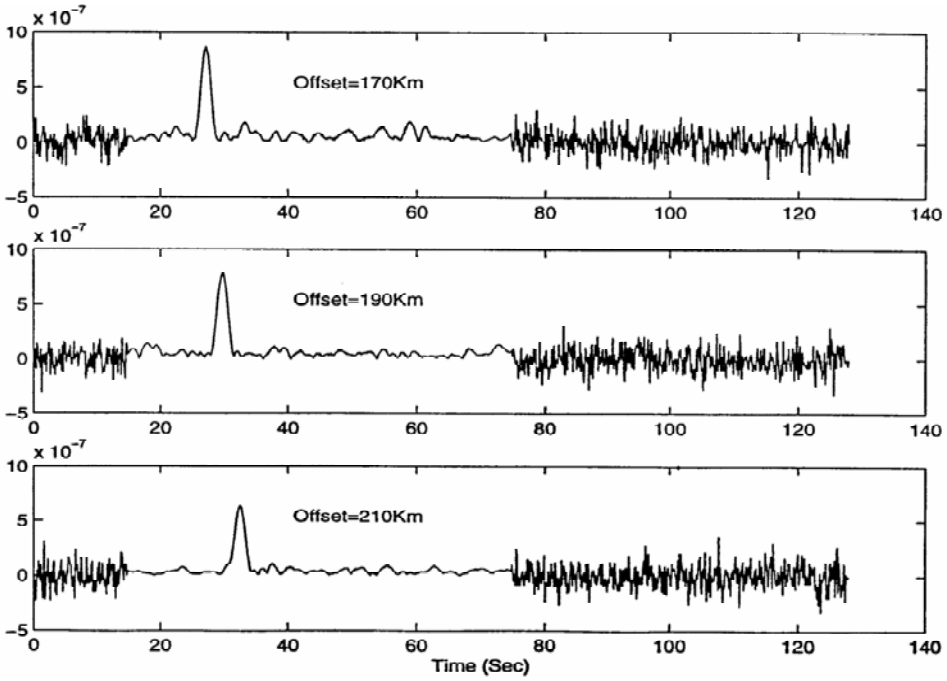

Figure 9. AMID output on noisy synthetic seismograms of Figure 8.

To further test the applicability of AMID method, a real example of OBS data have been used (Fig.10). The data shown in Figure 10 were recorded along Canadian border of the Atlantic Ocean. The airgun as an artificial seismic source has used to generate these data. The Ocean

Bottom Seismometer (OBS) is a self-contained data-acquisition system, which free falls to the see floor and records seismic signals. The result of AMID on this example is shown in Figure 11.

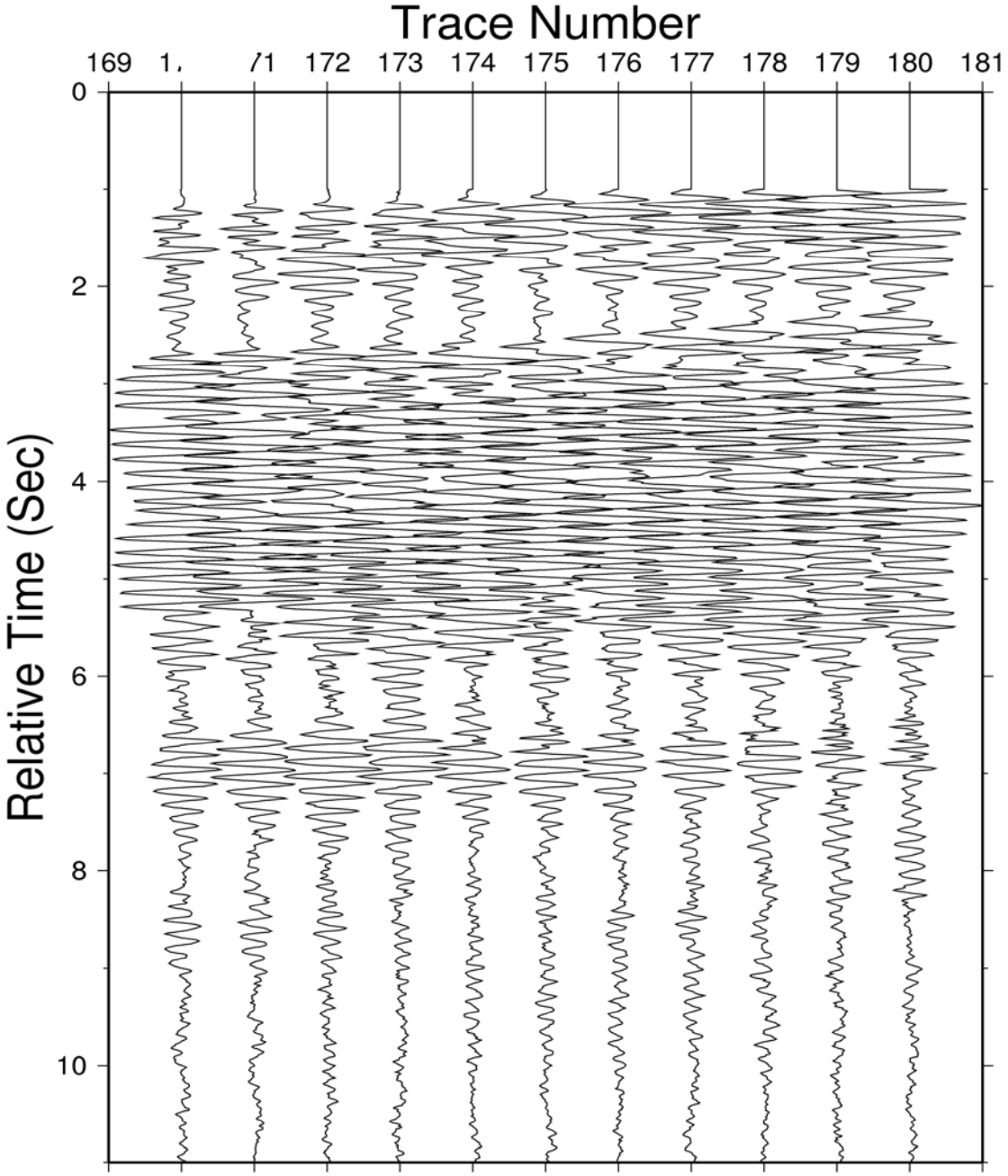

Figure 10. OBS data acquired along the Canadian margin of the Atlantic Ocean.

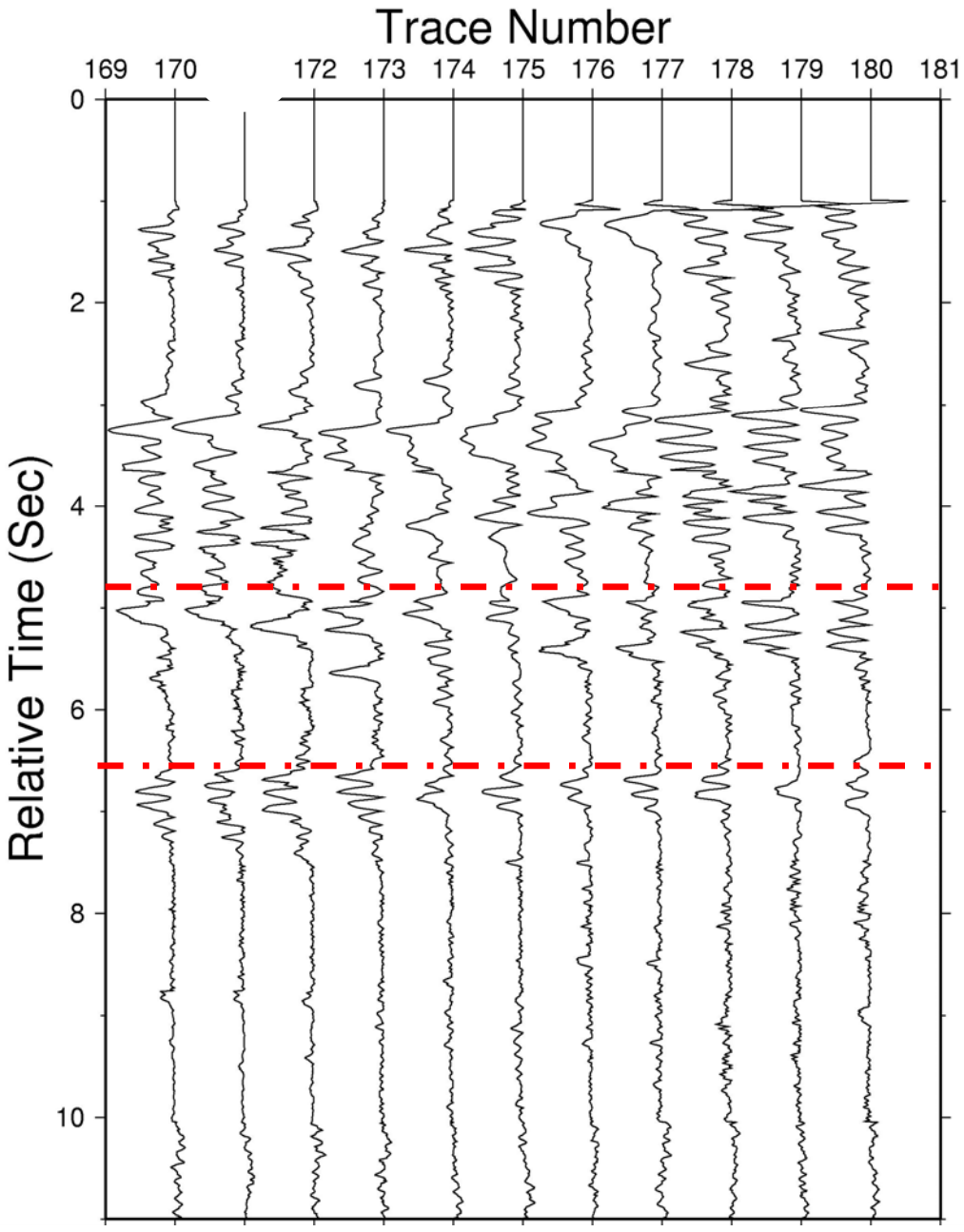

Figure 11. AMID output on seismograms of Figure 10.

It should be noted that the output of AMID are drown without including delay times. Figure 11 shows different phases in the maximum amplitude position of each phase on the processed seismic traces. Removing multiples at about 4.6 second made Moho reflection more visible in comparison with original seismic section of Figure 10. Therefore, AMID can be an effective tool for removing phase-shifted wavelets, random noise and multiples.

Discussions and Conclusion

Both synthetic and real data are assumed to contain distortion of phase shifted wavelets. The results of this study indicate the effectiveness of AMID technique to process crustal seismic data. Moreover, these numerical investigations show the potential power of the analytic formulation by AMID deconvolution, which like other methods, tends to compress the wavelet centered on its maximum amplitude. The only limitation of the method is closely spaced impulses. However, in the presence of phase-shifted wavelets, this limitation does not appear to be any more serious than those inherent in non-analytic techniques (e.g. scalar standard techniques). It was illustrated the importance of the introduced technique in recognizing reflectors as for example Moho. Therefore, it is realistic to apply AMID method in Signal/Noise improvement on seismic reflection data.

References

Aki, K., and Richards P.C. (1985) *Quantitative Seismology, Theory and methods*, vol.1: W-H Freeman and Co., 557p.

Arons, A. B., and Yennie, D. R. (1950) Phase distortion of Acoustic pulses obliquely reflected from a medium of higher sound velocity: J. Ac. Soc. Am., **22,** 231-237.

Claerbout J.F. (1978) Snell Waves, SEP-**15,** 57-72.

Herrmann, R.B. (1996) *An Overview of Synthetic Seismograms Computations and Computer Programs In Seismology*, Dept. of Earth and Atmospheric Sciences, Saint Louis University, Version 3.0.

Kim, H.J., and Marillier F. (1996) *Analytic minimum information deconvolution and its application to Ocean bottom seismometer data*, Geophys. Res. Letts, **23,** 1973 - 1976.

Levy, S., and Oldenburg D.W. (1982) *The deconvolution of phase - shifted wavelet*, Geophysics, **47,** 1285 -1294.

Robinson, E.A. (1999) *Seismic Inversion and Deconvolution*, Part B: Dual-Sensor Technology, Elsevier Sciences publication, 348p.

Sheriff, R., and Geldart, L. (1995) *Exploration Seismology*, Cambridge University Press.

Ulrych, T.J. and Walker C. (1982) *Analytic minimum entropy* deconvolution, Geophysics, **47,** 1295 – 1302.